RSC Advances

PAPER

View Article Online
View Journal | View Issue

Cite this: *RSC Adv.*, 2019, **9**, 9204

Preparation and characteristics of a novel PETN/TKX-50 co-crystal by a solvent/non-solvent method

Lei Xiao,[a] Shuangfeng Guo,[b] Hongping Su,[c] Bingwang Gou,[b] Qiaoe Liu,[c] Gazi Hao,[a] Yubing Hu,[a] Xiaohong Wang*[b] and Wei Jiang *[a]

In order to decrease the sensitivity and broaden the application of pentaerythritol tetranitrate (PETN), a novel energetic co-crystal composed of PETN and dihydroxylammonium 5,5′-bistetrazole-1,1′-diolate (TKX-50) with high energy and low sensitivity was successfully prepared through the solvent/non-solvent method. The morphology and structure of the as-prepared co-crystal were characterized by scanning electron microscopy (SEM), X-ray diffraction spectroscopy (XRD), X-ray photoelectron spectrometry (XPS), fourier transform infrared spectroscopy (FT-IR), Raman spectroscopy and high performance liquid chromatography (HPLC). The thermal decomposition properties were also analyzed by simultaneous thermogravimetry and differential scanning calorimetry (TG-DSC). The safety performance was judged by mechanical sensitivity tests. The SEM results revealed that the prepared new material was homogeneous with a mean granularity of 1 μm and the morphology was distinct from raw PETN and TKX-50. The XRD analysis indicated that a new crystalline formation appeared in the co-crystal which was quite different from the raw materials and their mixture. The XPS analysis showed peak shifts of C, N, O elements in the co-crystal. The FTIR spectra and Raman spectra suggested that hydrogen bond interactions existed between PETN and TKX-50 molecules. The molar ratio of PETN and TKX-50 was 1 : 1 determined by HPLC. There were two thermal decomposition peaks (194.1 °C and 261.3 °C) for the co-crystal at 20 °C min^{-1}, while the raw materials and mixture had only one. Besides, the activation energy of the co-crystal increased compared to the raw materials, indicating better thermal stability of the co-crystal. The impact sensitivity and friction sensitivity of the PETN/TKX-50 co-crystal were reduced compared to raw PETN, and were even better than for 1,3,5-trimethylene trinitramine (RDX). The results showed a prospective application of the prepared PETN/TKX-50 co-crystal in the future.

Received 23rd December 2018
Accepted 7th March 2019

DOI: 10.1039/c8ra10512j

rsc.li/rsc-advances

1. Introduction

Pentaerythritol tetranitrate (PETN) is a nitrate ester explosive with a detonation velocity of 8310 m s^{-1} at a density of 1.77 g cm^{-3}.[1] However, this explosive has not been widely applied in main charges or weapons because of its poor chemical stability in vacuum stability tests and high mechanical sensitivities. Thus, PETN is mostly used as an initiating or booster explosive.

So far, there have been many kinds of effective methods for decreasing the sensitivities of high-sensitivity explosives, such as surface coating,[2–4] improving crystal quality,[5–9] decreasing granularity,[1,10–13] *etc.* However, these methods still have some problems, such as decreased energy, complicated process, expensive equipment, *etc.* Therefore, a novel preparation technology for insensitive explosives is necessary. Co-crystal technology, which is widely used in the pharmaceutical industry, can improve bioavailability, stability and biocompatibility of pharmaceuticals with little effect on their chemical structure.[14–16] This technology has attracted more and more attention in military field. In recent years, quite a lot of energetic co-crystals have been prepared and excellent properties have been obtained.[17–23] J. P. Shen *et al.* prepared a kind of new co-crystal composed of HMX and TATB by the solvent/non-solvent method at room temperature and the impact sensitivity of the co-crystal explosive was relatively insensitive in contrast to HMX.[17] Bolton *et al.*[18] prepared a kind of co-crystal with a 2 : 1 molar ratio of 2,4,6,8,10,12-hexanitro-2,4,6,8,10,12-hexaazaiso-wurtzitane (CL-20) and 1,3,5,7-tetranitro-1,3,5,7-tetrazacy-clooctane (HMX). The small-scale impact drop test results showed that the sensitivity of co-crystal was lower than HMX due to the increased degree of hydrogen bond. H. Gao

[a]*National Special Superfine Powder Engineering Research Center of China, School of Chemical Engineering, Nanjing University of Science and Technology, Nanjing 210094, China. E-mail: superfine_jw@126.com; Fax: +86 25 84315042; Tel: +86 25 84315042*

[b]*Xi'an Modern Chemistry Research Institute, Xi'an 710065, China*

[c]*Research Institute, Gansu Yinguang Chemical Industry Group Co., Ltd., Baiyin, Gansu, 730900, China*

et al. produced HMX/NQ co-crystal with particle size under 500 nm by vacuum freeze drying method and found that the impact sensitivity of co-crystal was effectively reduced.[19] As can be seen from the above studies, the researchers adopt a co-crystal strategy that can balance two needs of high energy and low sensitivity of novel explosives.

As we know, dihydroxylammonium 5,5′-bistetrazole-1,1′-diolate (TKX-50) is a kind of promising energetic ionic salt prepared in 2012.[24,25] It shows excellent properties including higher detonation velocity (9698 m s^{-1}) than that of ε-CL-20 (9455 m s^{-1}) and lower mechanical sensitivities than that of RDX.[26] It has the potential advantage as a low sensitive component in the co-crystal explosive.

In this study, a kind of novel superfine co-crystal explosive with high energy and low sensitivity was prepared by solvent/non-solvent method, in which PETN was used as the sensitive ingredient and TKX-50 was selected as the insensitive ingredient. The chemical structures of PETN and TKX-50 are presented in Fig. 1.

2. Experimental

2.1 Materials

Raw PETN and TKX-50 were provided by Gansu Yinguang Chemical Industry Group Co., Ltd. (China). *N*,*N*-Dimethylformamide (DMF), AR, was purchased from Sinopharm Chemical Reagent Co., Ltd. (China). Chloroform, AR, was purchased from Shanghai Lingfeng Chemical Reagent Co., Ltd. (China).

2.2 Preparation of PETN/TKX-50 co-crystal

The PETN/TKX-50 co-crystal was prepared by the solvent/non-solvent method. Firstly, 0.158 g of PETN and 0.118 g TKX-50 (molar ratio 1 : 1) were weighed and added into 20 mL of DMF. The two kinds of explosives were dissolved after being stirred for 30 min under ultrasonic condition and at 60 °C. Secondly, the formed transparent solution was dropped into the 150 mL of chloroform at the rate of 0.5 mL min^{-1} under 1000 rpm. After that, the mixed solution was kept stirring for 1 h followed by filtered, and then dried through a vacuum drying process for 3 h in order to improve drying efficiency. At last, the white PETN/TKX-50 co-crystal powders were obtained.

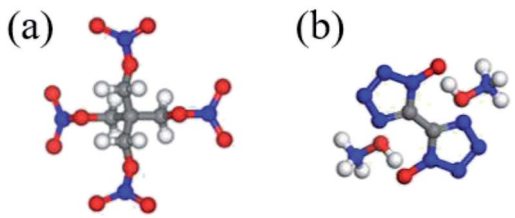

Fig. 1 Chemical structures of (a) PETN, $C_5H_8N_4O_{12}$ and (b) TKX-50, $C_2H_8N_{10}O_4$.

2.3 Equipments and conditions

The morphology and size of samples were characterized by a field emission scanning electron microscope (FE-SEM, Hitachi S-4800 II, Japan) operating at 10–15 kV.

The crystal structures of samples were investigated by an X-ray diffractometer (XRD, Bruker Advance D8) with the use of Cu Kα radiation at 40 kV and 30 mA. Images were integrated from 5° to 80° with a step size of 0.05° and each peak was scanned twice.

The structures of samples were characterized by an ESCALAB 250Xi X-ray photoelectron spectrometer (XPS, Thermo Fisher Scientific, UK) with a monochromatic Al Kα radiation source (energy 1486.68 eV) at 164 W (10.8 mA and 15.2 kV) and a spot size approximately 0.5 mm in diameter. During analysis vacuum was maintained $<2 \times 10^{-9}$ mbar. The electron energy analyser was operated with a pass energy of 20 eV enabling high resolution of the spectra to be obtained. The step size of 0.05 eV was employed and each peak was scanned twice.

Fourier transform infrared spectroscopy (FT-IR) analyses of samples were performed on an American Thermofisher Scientific Nicolet 6700 infrared spectrometer (iodine bromide tablet). The data were collected from 500 to 4000 cm^{-1}.

Raman spectra of samples were measured on a LabRAM HR Evolution Raman spectrometer (HORIBA JY Co., Ltd., French) with working range from 4000 to 10 cm^{-1}. And the excitation source was a 532 nm laser (2.33 eV).

The molar ratio of PETN and TKX-50 in co-crystal was tested through high performance liquid chromatography (HPLC) analysis on an Agilent 1260 HPLC system.

The thermogravimetric analysis (TG) and differential scanning calorimetry (DSC) of samples were carried out with a SDT Q600 thermal analyzer (TA Instruments Co., Ltd., America). The weight of samples was about 0.5–1 mg and placed in an alumina crucible. All the tests were performed under four heating rates of 5, 10, 15 and 20 °C min^{-1} from 50 to 400 °C. The high-purity nitrogen was used with flow rate of 50 mL min^{-1}.

The impact sensitivities of samples were tested with a HGZ-1 impact instrument. A certain height from which a 5 kg hammer dropped and resulted in an initiation event in 50% of the trials was recorded. The characteristic drop height (H_{50}) was calculated according to the recorded height data of 25 tests to represent impact sensitivity. And each lot was tested three times to obtain a mean value and a standard deviation.

The friction sensitivities of samples were tested with a WM-1 friction instrument. In each test, whether an explosive event occurred or not was recorded when a weighted pendulum scraped across the sample (20 mg), and an explosion probability (P, %) was obtained. Each lot was tested for three times to obtain a mean value.

3. Results and discussion

The morphology and particle sizes of raw PETN, raw TKX-50 and PETN/TKX-50 co-crystal were characterized by SEM, and the results are shown in Fig. 2.

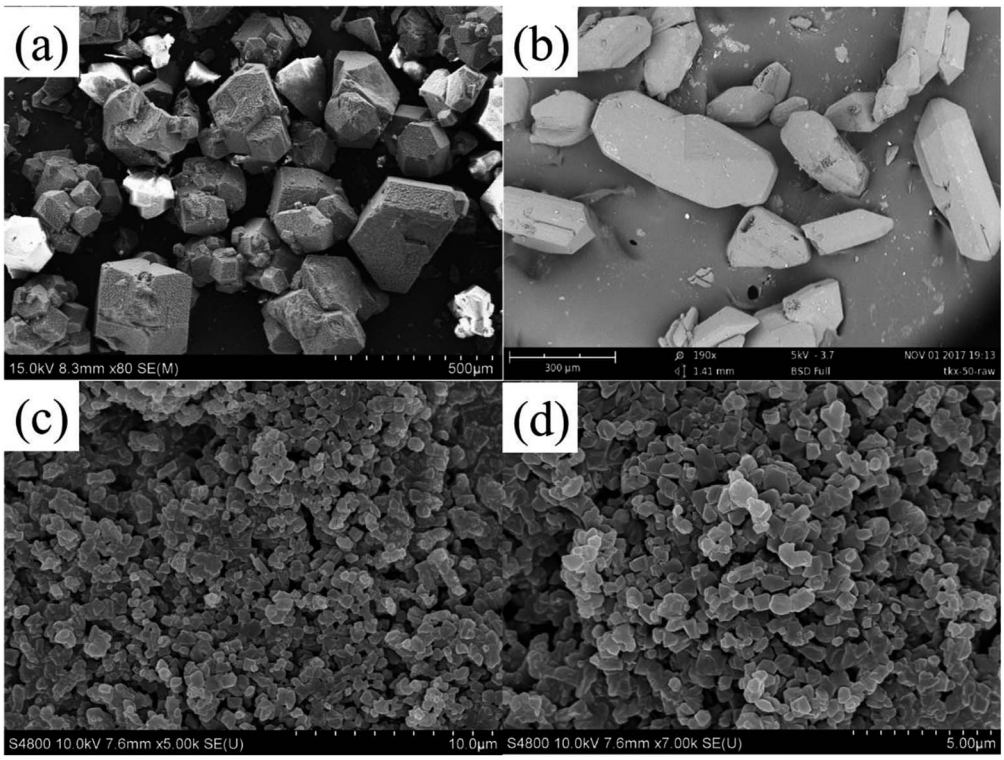

Fig. 2 SEM images of (a) raw PETN, (b) raw TKX-50, (c) and (d) PETN/TKX-50 co-crystal.

As it can be seen from Fig. 2a, the raw PETN particles represented bulk crystal structure with a wide distribution range of granularity from 100 μm to 500 μm. Fig. 2b showed the irregular polyhedron structures of raw TKX-50 with the shapes of short rod and cambiform, and the particles were over 100 μm in a wider range. While the images of co-crystal in Fig. 1c and d exhibited different morphology. The particle size of co-crystal was uniform and the average granularity was about 1 μm with smooth and integrated surfaces. Thus, the as-prepared co-crystal would show some advantages in the low mechanical sensitivities and good formability in the charge process compared with raw PETN and TKX-50.

The crystal structures of prepared PETN/TKX-50 co-crystal was analysed *via* XRD as well as raw PETN, raw TKX-50 and PETN/TKX-50 mixture. The resulting XRD patterns are performed in Fig. 3. It can be clearly observed that the XRD pattern of co-crystal was distinct from other three samples. The new diffraction angles located at 8.19°, 9.60°, 23.74° and some weak peaks in the range of 20–22.5° appeared in PETN/TKX-50 co-crystal. Some of peaks for raw PETN and TKX-50 disappeared or were weaken, such as 37.88° and the peaks in the range of 51–55° for PETN, 15.38°, 17.93° and 28.01° for TKX-50. Besides, some of the peaks were obviously strengthened, such as 13.13°, 18.67°, 26.59° for PETN and 26.89° for TKX-50. The above differences enabled it easy to distinguish the prepared PETN/TKX-50 co-crystal from raw PETN, raw TKX-50 and PETN/TKX-50 mixture. The unique XRD patterns of the co-crystal indicated that it was a new kind of substance instead of the simple mixture of raw materials.

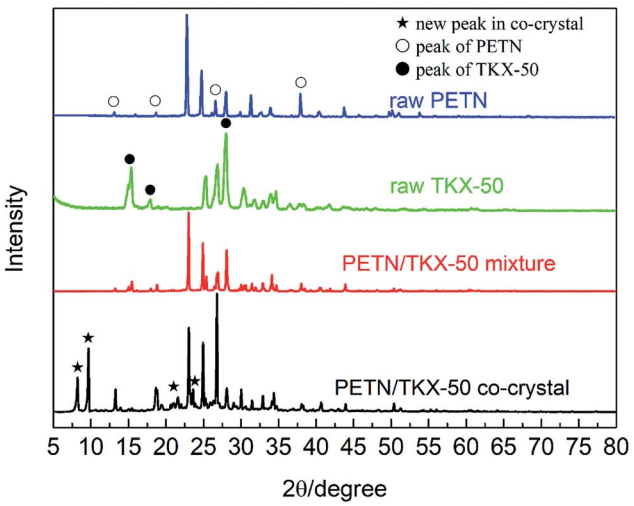

Fig. 3 XRD spectra of raw PETN, raw TKX-50, PETN/TKX-50 mixture and PETN/TKX-50 co-crystal.

The structures of raw PETN, raw TKX-50, PETN/TKX-50 mixture and PETN/TKX-50 co-crystal were analysed by XPS. The resulting XPS spectra of C, N and O of the above samples are performed in Fig. 4 and the peak values are listed in Table 1. According to Fig. 4a and b, it can be clearly seen that the XPS spectra of C, N, O in PETN and TKX-50 were different due to their different molecular structures. And the XPS spectra of C, N and O in PETN/TKX-50 mixture in Fig. 4c was simple superposition of PETN and TKX-50, which revealed that there was no

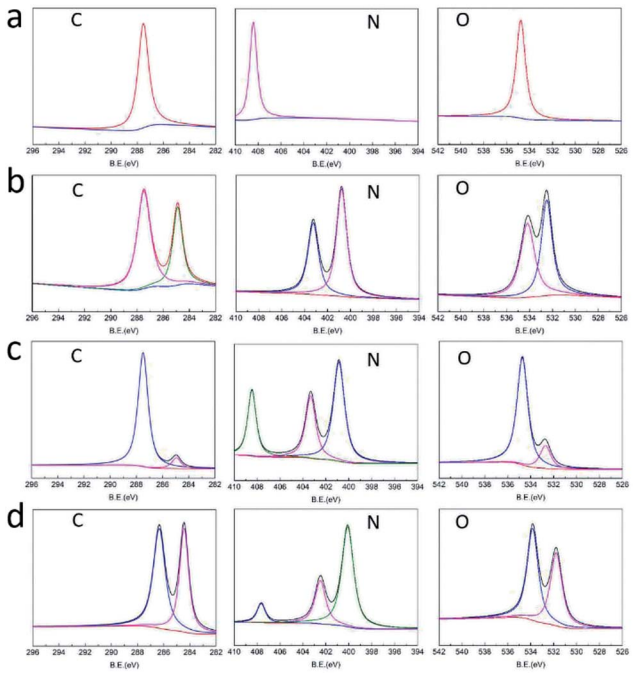

Fig. 4 XRS spectra of (a) raw PETN, (b) raw TKX-50, (c) PETN/TKX-50 mixture and (d) PETN/TKX-50 co-crystal.

Table 1 XPS peak values of C, N and O of raw PETN, raw TKX-50, PETN/TKX-50 mixture and PETN/TKX-50 co-crystal

Samples	C 1s (eV)		N 1s (eV)			O 1s (eV)	
PETN	287.5	—	408.4	—	—	534.7	—
TKX-50	287.5	284.9	—	403.3	400.8	534.2	532.5
Mixture	287.5	284.9	408.4	403.3	400.9	534.7	532.7
Crystal	286.3	284.4	407.6	402.5	400.1	533.8	531.8

structure change in mixture. But the co-crystal showed difference peak positions. Comparing the peak values of PETN/TKX-50 mixture and co-crystal listed in Table 1, it can be found that the C peaks in co-crystal were shifted to 286.3 eV and 284.4 eV from 287.5 eV and 284.9 eV of C peaks in mixture. The N peaks in co-crystal were shifted to 407.6 eV, 402.5 eV and 400.1 eV from 408.4 eV 403.3 eV and 400.9 eV of N peaks in mixture. The O peaks at 534.7 eV and 532.7 eV in mixture were shifted to 533.8 eV and 531.8 eV in co-crystal. The above XPS analyses revealed that new bond interaction existed in prepared PETN/TKX-50 co-crystal which was different from simple mixture of PETN and TKX-50. The FTIR spectra of raw PETN, raw TKX-50, PETN/TKX-50 mixture and PETN/TKX-50 co-crystal are shown in Fig. 5. Generally speaking, the IR spectrum of co-crystal was similar to the PETN/TKX-50 mixture which was the simple superposition of raw PETN and raw TKX-50. And the main absorption peaks of raw PETN and raw TKX-50 existed in the spectrum of co-crystal, revealing that the as-prepared co-crystal was composed of PETN and TKX-50. However, some differences also appeared by comparing the spectrum of co-crystal and raw materials more or less. For example, the peak at 1641.95 cm^{-1} which represented the asymmetric stretching vibration of $-NO_2$

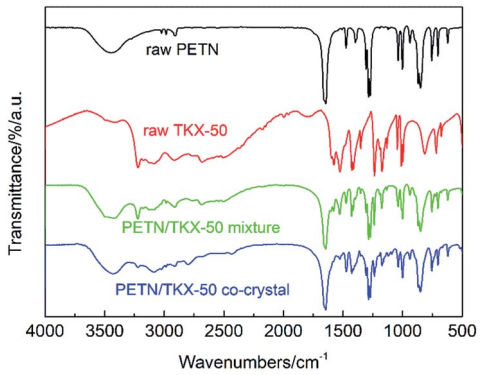

Fig. 5 FTIR spectra of raw PETN, raw TKX-50, PETN/TKX-50 mixture and PETN/TKX-50 co-crystal.

in PETN was shifted to 1648.14 cm^{-1}. The peak at 1398.51 cm^{-1} in TKX-50 was weakened. The peak at 1476.91 cm^{-1} which was corresponded to the in-plane bending vibration of C–H in PETN was shifted to 1472.78 cm^{-1}. The peak at 3222.23 cm^{-1} which was attributed to the stretching vibration of NH_3^+ in TKX-50 was shifted to 3226.36 cm^{-1}. The peaks at 1578.01 cm^{-1} and 1526.42 cm^{-1} (bending vibration of NH_3^+) in TKX-50 were weakened. Based on the above analyses, it can be conjectured that there may exist hydrogen bond interactions betweenPETN and TKX-50.

Besides FTIR analyses, the Raman spectroscopy is also a meaningful method for the distinction between prepared co-crystal and raw materials. And the Raman spectra are presented in Fig. 6. Similar to the IR analyses, the Raman spectra of PETN/TKX-50 mixture and co-crystal contained the characteristic vibrational bands of both PETN and TKX-50, but there were still some peak shifts appearing in the curve of co-crystal. For example, the bands at 2985.01 cm^{-1} and 3034.2 cm^{-1} which were corresponded to C–H stretching in PETN shifted to 2986.31 cm^{-1} and 3022.91 cm^{-1}, respectively. Furthermore, the bands at 1003.47 cm^{-1}, 1240.6 cm^{-1} and 1615.91 cm^{-1} in TKX-50 shifted to 1006.77 cm^{-1}, 1238.45 cm^{-1} and 1617.45 cm^{-1}, respectively. More band shifts have been marked and can be observed in Fig. 6. These changes above-mentioned could be attributed to the hydrogen bond interactions between the PETN and TKX-50 molecules.

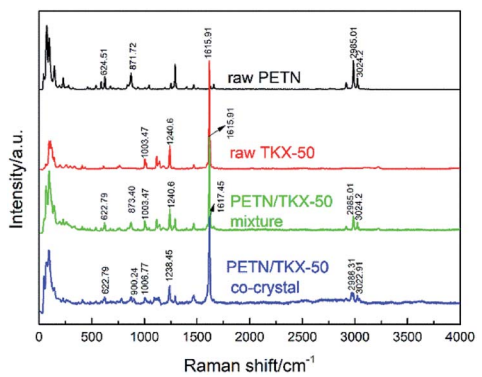

Fig. 6 Raman spectra of raw PETN, raw TKX-50, PETN/TKX-50 mixture and PETN/TKX-50 co-crystal.

Besides, the HPLC results showed that the mass percentages of PETN and TKX-50 in prepared co-crystal were about 57.2% and 42.8%, respectively, which was corresponding to the molar ratio of 1 : 1. The HPLC result revealed that the PETN/TKX-50 co-crystal was exactly prepared in molar ratio of 1 : 1.

The thermodynamics behaviors of PETN/TKX-50 co-crystal were examined by using simultaneous TG-DSC measurements. The different TG and DSC curves of raw PETN, raw TKX-50 and PETN/TKX-50 mixture and PETN/TKX-50 co-crystal at 20 °C min^{-1} are shown in Fig. 7, and the DSC traces of these four kinds of samples at different heating rates of 5, 10, 15 and 20 °C min^{-1} are shown in Fig. 8.

It can be observed from Fig. 7 that the thermal behavior of as-prepared co-crystal was distinct from the raw materials and mixture. TG curve of co-crystal was similar to that of raw TKX-50 and the mixture with two weight loss steps while the raw PETN had only one. However, the differences can be obvious based on the DSC curves in Fig. 7. There was an endothermic peak at about 148.4 °C and an exothermic peak at 216.9 °C followed during the decomposition of PETN. When raw TKX-50 was decomposed, there was only an obvious and sharp exothermic peak with the exothermic peak temperature of 256.2 °C, and a weak acromion was accompanied around 272.6 °C which was in accordance with TG trace. It can be observed that there was only one exothermic peak at 183.7 °C in the DSC curve of PETN/TKX-50 mixture. However, the DSC trace of co-crystal revealed something different. With the rise of temperature, there was an endothermic peak at about 144.8 °C ahead of that of raw PETN. And then, the first exothermic peak at 194.1 °C (DP1) appeared with the second exothermic peak at 261.3 °C (DP2) followed. These differences illustrated that this is the target co-crystal instead of a mixture. In fact, TKX-50 was a kind of energetic ionic salt and it had poor compatibility with some other energetic materials, such as TNT, RDX, CL-20, NC[27,28] which limited its wide application. Herein, it can be also found that the compatibility of TKX-50 and PETN was not good. When the two explosives were mixed, they would react with each other, resulting in great advance of exothermic reaction. While the co-crystal seemed to have good effect on the compatibility which could be attributed to the formation of hydrogen bonds. Thus the co-crystal technology may be a possible way to improve compatibility and broaden the application of two or more energetic materials with poor compatibility.

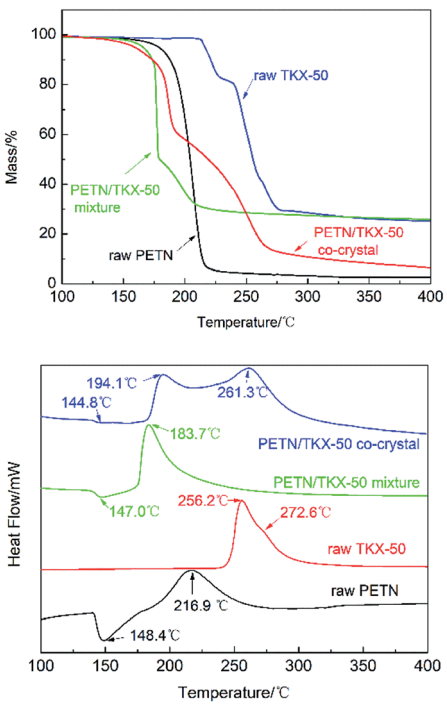

Fig. 7 TG and DSC curves of raw PETN, raw TKX-50, PETN/TKX-50 mixture and PETN/TKX-50 co-crystal at 20 °C min^{-1}.

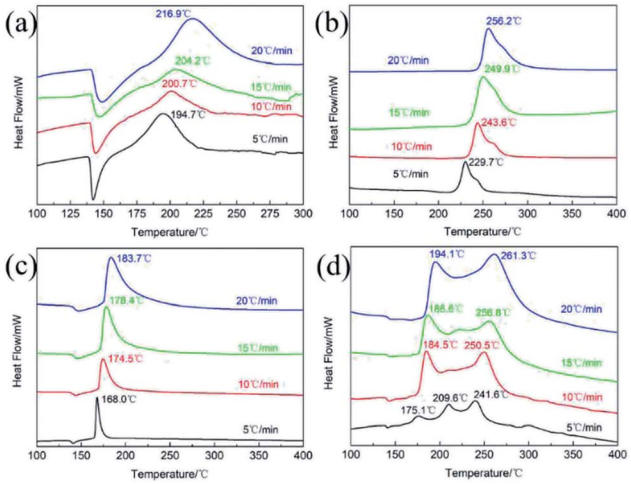

Fig. 8 DSC curves of (a) raw PETN, (b) raw TKX-50, (c) PETN/TKX-50 mixture and (d) PETN/TKX-50 co-crystal at different heating rates of 5, 10, 15 and 20 °C min^{-1}.

For further study, a detailed evaluation of the thermodynamics was performed. The kinetic parameters for decomposition of different samples are calculated according to the exothermic peak temperature dependence as a function of heating rate (Kissinger correlation).[29] The activation enthalpy (ΔH), activation free energy (ΔG), and activation entropy (ΔS) for the thermal decomposition of raw PETN, raw TKX-50 and PETN/TKX-50 mixture and PETN/TKX-50 co-crystal are calculated on the basis of eqn (2)–(4), respectively. And the resulted data are tabulated in Table 2.

$$\ln\left(\frac{\beta}{T_P^2}\right) = -\frac{E_a}{RT_P} + \ln\left(\frac{AR}{E_a}\right) \quad (1)$$

where β is the heating rate in degrees celsius per minute, T_P is the maximum exothermic peak temperature, R is the ideal gas constant, E_a is the activation energy, A is the pre-exponential factor.

$$A\exp\left(-\frac{E_a}{RT_P}\right) = \frac{K_B T_P}{h}\exp\left(-\frac{\Delta G}{RT_P}\right) \quad (2)$$

$$\Delta H = E_a - RT_P \quad (3)$$

$$\Delta G = \Delta H - T_P\Delta S \quad (4)$$

Table 2 DSC peak temperatures and kinetic parameters for raw PETN, raw TKX-50, PETN/TKX-50 mixture and PETN/TKX-50 co-crystal at 5, 10, 15 and 20 °C min^{-1}

Samples	$T_{P,\beta}$ (°C)				E_a (kJ mol^{-1})	ΔH (kJ mol^{-1})	ΔG (kJ mol^{-1})	ΔS (J K^{-1} mol^{-1})
	$T_{P,5}$	$T_{P,10}$	$T_{P,15}$	$T_{P,20}$				
Raw PETN	194.7	200.7	204.2	216.9	104.4	100.3	137.9	−76.6
Raw TKX-50	229.7	243.6	249.9	256.2	108.4	104.0	150.5	−87.9
PETN/TKX-50 mixture	168.0	174.5	178.4	183.7	143.3	139.5	126.8	27.8
DP1	175.1	184.5	186.6	194.1	123.2	119.4	130.6	−24.0
DP2	241.6	250.5	256.8	261.3	152.0	147.6	150.5	−5.4

where K_B is the Boltzmann constant ($K_B = 1.381 \times 10^{-23}$ J K^{-1}); h is the Planck constant ($h = 6.626 \times 10^{-34}$ J s); T_P is the exothermic peak temperature in the DSC curve at a heating rate of 20 °C min^{-1}.

As shown in Table 2 that E_a and ΔH values of DP1 and DP2 were higher than raw PETN and raw TKX-50, respectively, which revealed that the prepared co-crystal needed more energy to decompose. Besides, all the ΔG data were positive, representing that the activating reaction were not spontaneous. The thermodynamic results indicated that thermal stability of PETN/TKX-50 co-crystal was superior to raw PETN and TKX-50.

High mechanical sensitivities of PETN are the major limitation for its wide applications, which is the fundamental problem to be solved in this study using co-crystal technology. Hence, the impact sensitivities and friction sensitivities of raw PETN, raw TKX-50, PETN/TKX-50 mixture and PETN/TKX-50 co-crystal were tested. Besides, the mechanical sensitivities of raw RDX were also analysed to make a comparison. The results are tabulated in Table 3.

It can be seen clearly from Table 3 that the as-prepared PETN/TKX-50 co-crystal showed good mechanical sensitivities, compared with raw PETN. Raw TKX-50 itself was a kind of explosive with good sensitivity. Thus, the mechanical sensitivities of PETN/TKX-50 mixture were slightly decreased compared with raw PETN. While the H_{50} of co-crystal was increased from 14.5 cm of raw PETN to 42.2 cm, indicating that the impact sensitivity of co-crystal had a decrease of about 191%. Besides, the standard deviation S of co-crystal was only 0.06, smaller than 0.12 of raw PETN and 0.14 of raw TKX-50, which revealed that the ignition stability of co-crystal was better than raw materials. The friction sensitivity of co-crystal was also reduced from 68% of raw PETN to 12% which was even lower than 28% of raw TKX-50. On the other hand, the sensitivities of co-crystal were much lower than raw RDX according to Table 3. The reason for insensitivity of as-prepared co-crystal could be ascribed to the formation of intermolecular hydrogen bonds between PETN and TKX-50 which lead to a more close packing of the molecules and reduce the defects inside new crystals.[30] At the same time, the as-prepared co-crystal has a uniform particle size distribution of about 1 μm in a relatively smooth surface, which was another reason for the low sensitivities of co-crystal.[31–33] Thus, it can be concluded that the PETN/TKX-50 co-crystal is a kind of new energetic material with high energy and low sensitivity.

Table 3 Impact sensitivities and friction sensitivities of raw PETN, raw TKX-50, PETN/TKX-50 mixture, PETN/TKX-50 co-crystal and raw RDX

Samples	Impact sensitivity		Friction sensitivity
	H_{50}, cm	S	P, %
Raw PETN	14.5	0.12	68
Raw TKX-50	55.4	0.14	28
PETN/TKX-50 mixture	20.7	0.11	60
PETN/TKX-50 co-crystal	42.2	0.06	12
Raw RDX	21.5	0.12	36

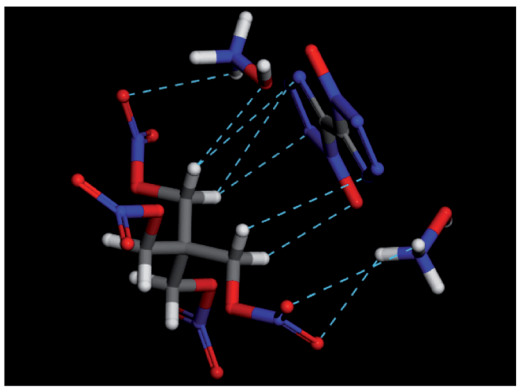

Fig. 9 Possible hydrogen bonds (dashed) between PETN and TKX-50.

In the end, the computational tool Material Studio was also used to simulate the possible hydrogen bonds between PETN and TKX-50 molecules. The Forcite module was chosen for mechanical optimization of single molecule. The result is shown in Fig. 9. It can be seen that the intermolecular hydrogen bonds were formed between $-NO_2$ group in PETN and NH_3OH^+ in TKX-50. Thus, this kind of PETN/TKX-50 co-crystal shows good sensitivities and has a potential application in the future due to the hydrogen bonds.

4. Conclusions

(1) A kind of superfine PETN/TKX-50 co-crystal with a molar ratio of 1 : 1 was successfully prepared by solvent/non-solvent method and showed different morphology from raw materials;

(2) The XRD, XPS, FTIR and Raman further confirmed the new formation of co-crystal structure and the hydrogen bond interactions between PETN and TKX-50.

(3) The thermal stability of co-crystal was proved to be better than raw materials. And the mechanical sensitivities showed that the prepared co-crystal was more insensitive than raw PETN and was close to raw TKX-50, even better than raw RDX. This work will help extend the practical application of PETN and TKX-50. In addition, the solvent/non-solvent method will do good to the rapid and massive preparation of novel energetic co-crystals with high energy and low sensitivity, which certainly will accelerate the wide applications of co-crystals.

Conflicts of interest

There are no conflicts to declare.

Acknowledgements

This work was financially supported by National Natural Science Foundation of China (No. 51606102, No. 21805139), the Fundamental Research Funds for the Central Universities (No. 30918011312), Basic Product Innovation Technology Research Project of Explosives and Youth Scientific and Technological Innovation Project (QKCZ201713).

Notes and references

1 X. L. Song, Y. Wang and C. W. An, *AIP Adv.*, 2018, **8**, 065009.
2 K. Cowey, S. Day and R. Fryer, *Propellants, Explos., Pyrotech.*, 1985, **10**, 61–64.
3 A. K. Nandi, M. Ghosh, V. B. Sutar and R. K. Pandey, *Cent. Eur. J. Energ. Mater.*, 2012, **9**, 119–130.
4 Z. Ma, B. Gao, P. Wu, *et al.*, *RSC Adv.*, 2015, **5**, 21042–21049.
5 R. M. Doherty and D. S. Watt, *Propellants, Explos., Pyrotech.*, 2008, **33**, 4–13.
6 L. Borne, J. Mory and F. Schlesser, *Propellants, Explos., Pyrotech.*, 2008, **33**, 37–43.
7 A. E. D. M. van der Heijden, R. H. B. Bouma and A. C. van der Steen, *Propellants, Explos., Pyrotech.*, 2004, **29**, 304–313.
8 H. Kröber and U. Teipel, *Propellants, Explos., Pyrotech.*, 2008, **33**, 33–36.
9 H. Czerski and W. G. Proud, *J. Appl. Phys.*, 2007, **102**, 1–8.
10 N. Radacsi, A. I. Stankiewicz, Y. L. M. Creyghton, A. E. D. M. van der Heijden and J. H. ter Horst, *Chem. Eng. Technol.*, 2011, **34**, 624–630.
11 Y. Bayat, M. Zarandi, M. A. Zarei, R. Soleyman and V. Zeynali, *J. Mol. Liq.*, 2014, **193**, 83–86.
12 Y. Bayat and V. Zeynali, *J. Energ. Mater.*, 2011, **29**, 281–291.
13 X. D. Guo, G. Ouyang, J. Liu, Q. Li, L. X. Wang, Z. M. Gu and F. S. Li, *J. Energ. Mater.*, 2015, **33**, 24–33.
14 N. Qiao, M. Li, W. Schlindwein, *et al.*, *Int. J. Pharm.*, 2011, **419**, 1–11.
15 S. Li, T. Yu, Y. Tian, *et al.*, *Mol. Pharm.*, 2018, **15**, 3741–3754.
16 P. Panzade and G. R. Shendarkar, *Curr. Drug Delivery*, 2017, **13**, 1097–1105.
17 J. P. Shen, X. H. Duan, Q. P. Luo, *et al.*, *Cryst. Growth Des.*, 2011, **11**, 1759–1765.
18 O. Bolton, L. R. Simke, P. F. Pagoria and A. J. Matzger, *Cryst. Growth Des.*, 2012, **12**, 4311–4314.
19 H. Gao, Q. Wang, X. Ke, *et al.*, *RSC Adv.*, 2017, **7**, 46229–46235.
20 H. F. Xu, X. H. Duan, H. Z. Li, *et al.*, *RSC Adv.*, 2015, **5**, 95764–95770.
21 H. Gao, P. Du, X. Ke, *et al.*, *Propellants, Explos., Pyrotech.*, 2017, **42**, 889–895.
22 J. J. Tao, B. Jin, S. J. Chu, *et al.*, *RSC Adv.*, 2018, **8**, 1784–1790.
23 C. Huang, J. J. Xu, X. Tian, *et al.*, *Cryst. Growth Des.*, 2018, **18**, 2121–2128.
24 N. Fischer, D. Fischer, T. Klapotke, *et al.*, *J. Mater. Chem.*, 2012, **22**, 20418–20422.
25 Z. P. Lu, X. G. Xue, L. Y. Meng, *et al.*, *J. Phys. Chem. C*, 2017, **121**, 8262–8271.
26 V. P. Sinditskii, S. A. Filatov, V. I. Kolesov, *et al.*, *Thermochim. Acta*, 2015, **614**, 85–92.
27 H. F. Huang, Y. M. Shi, J. Yang, *et al.*, *J. Energ. Mater.*, 2015, **33**, 66–72.
28 F. Q. Bi, X. Z. Fan, X. L. Fu, *et al.*, *Guti Huojian Jishu*, 2014, **37**, 214–218.
29 H. E. Kissinger, *Anal. Chem.*, 1957, **29**, 1702–1706.
30 H. Gao, W. Jiang, J. Liu, *et al.*, *J. Energ. Mater.*, 2017, **35**, 1–9.
31 X. L. Song, Y. Wang, C. W. An, *et al.*, *J. Hazard. Mater.*, 2008, **159**, 222–229.
32 V. Stepanov, V. Anglade, W. A. B. Hummers, *et al.*, *Propellants, Explos., Pyrotech.*, 2011, **36**, 240–246.
33 J. Liu, W. Jiang, Q. Yang, J. Song, G. Z. Hao and F. S. Li, *Def. Technol.*, 2014, **10**, 184–189.